

## Quasicrystals in a monodisperse system

Anna Skibinsky,<sup>1,2</sup> Sergey V. Buldyrev,<sup>1</sup> Antonio Scala,<sup>1</sup> Shlomo Havlin,<sup>1,3</sup> and H. Eugene Stanley<sup>1</sup>

<sup>1</sup>*Center for Polymer Studies and Department of Physics, Boston University, Boston, Massachusetts 02215*

<sup>2</sup>*Department of Chemistry, Boston University, Boston, Massachusetts 02215*

<sup>3</sup>*Department of Physics, Bar-Ilan University, Ramat-Gan 52900, Israel*

(Received 9 November 1998; revised manuscript received 21 May 1999)

We investigate the formation of a two-dimensional quasicrystal in a monodisperse system, using molecular dynamics simulations of hard-sphere particles interacting via a two-dimensional square-well potential. We find that more than one stable crystalline phase can form for certain values of the square-well parameters. Quenching the liquid phase at a very low temperature, we obtain an amorphous phase. By heating this amorphous phase, we obtain a quasicrystalline structure with fivefold symmetry. From estimations of the Helmholtz potentials of the stable crystalline phases and of the quasicrystal, we conclude that the observed quasicrystal phase can be the stable phase in a specific range of temperatures. [S1063-651X(99)07909-X]

PACS number(s): 05.70.Ce, 61.44.Br, 05.20.-y

### I. INTRODUCTION

Stable quasicrystalline phases are typically found in binary mixtures [1], where the various arrangements of the two components contribute to the degeneracy of the local environments [2], allowing a quasicrystalline phase to be entropy stabilized [3]. With one notable exception [4], previous studies did not support the existence of a stable quasicrystalline phase in a monodisperse system interacting with a simple potential [5,6].

We study a simple model that allows us to estimate the crystal and quasicrystal entropies and thereby study the Helmholtz potentials of the crystals and quasicrystal. The ground state of this system is a periodic crystal, yet we explore the possibility that the quasicrystalline configuration is the equilibrium state in a certain temperature regime. Although quasicrystals do not have long-range translational symmetry, they do have recurring local environments that, in our model, resemble the basic cells of the stable crystalline phases. From the entropies of the stable crystalline phases and by estimating the configurational entropy of the quasicrystal, we infer that the quasicrystal may be an equilibrium state. We observe sharpening of fivefold diffraction peaks when the starting amorphous phase is annealed. In two dimensions, fivefold diffraction peaks pertain to crystallographically disallowed point groups, which characterize quasicrystals [7].

### II. MD METHODS

To study quasicrystalline stability in a monodisperse system, we perform molecular-dynamics (MD) simulations of a two-dimensional model of hard spheres interacting with an attractive square-well (SW) potential [Fig. 1]. The simplicity of this SW potential allows us to study the fundamental characteristics of the system. By tuning the width of the SW potential, we can control the local geometric configurations formed by the particles. The structures of the crystalline and quasicrystalline phases can thus be clearly defined and analyzed.

We perform MD simulations at constant number of par-

ticles, volume, and temperature, using a standard collision event list algorithm [8] to evolve the system, while we use a method similar to the Berendsen method to achieve the desired temperature [9]. The depth of the potential well is  $\epsilon = -1.0$ . Energies are measured in units of  $\epsilon$ , temperature is measured in units of energy divided by the Boltzmann constant,  $\epsilon/k_B$ , and the mass of the particle is  $m = 1$ . We choose the value of the hard-core distance to be  $a = 10$ , and the ratio of the attractive distance  $b$  to the hard-core distance  $a$ , to be  $b/a = \sqrt{3}$ . Since the diagonal distance between two corners of a square is  $\sqrt{2}$  times the length of one side, choosing  $b/a = \sqrt{3}$  favors the formation of a square crystal lattice where each particle interacts with eight neighbors [Fig. 2(a)]. This constraint inhibits the formation of a triangular crystal, which would form at low temperatures if  $b/a > \sqrt{3}$  or at high densities.

### III. CRYSTAL AND AMORPHOUS PHASES

Studying the behavior of the system at low temperatures, we observe the formation of local structures similar to that shown in Fig. 2. These structures constitute local environments [2] that can reproduce crystallographically allowed symmetry if translationally ordered. First, we consider the

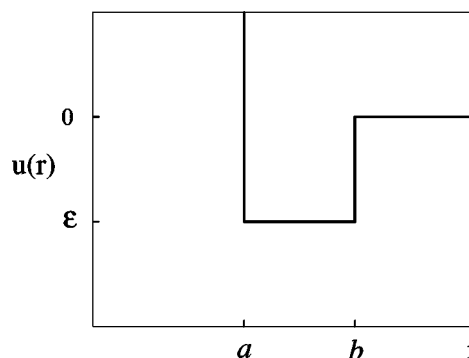


FIG. 1. Square-well potential. The ratio of the attractive distance  $b$  to the hard-core repulsive distance  $a$  is  $b/a = \sqrt{3}$ . The depth of the square-well  $\epsilon = -1.0$  is the interaction energy per pair of particles.

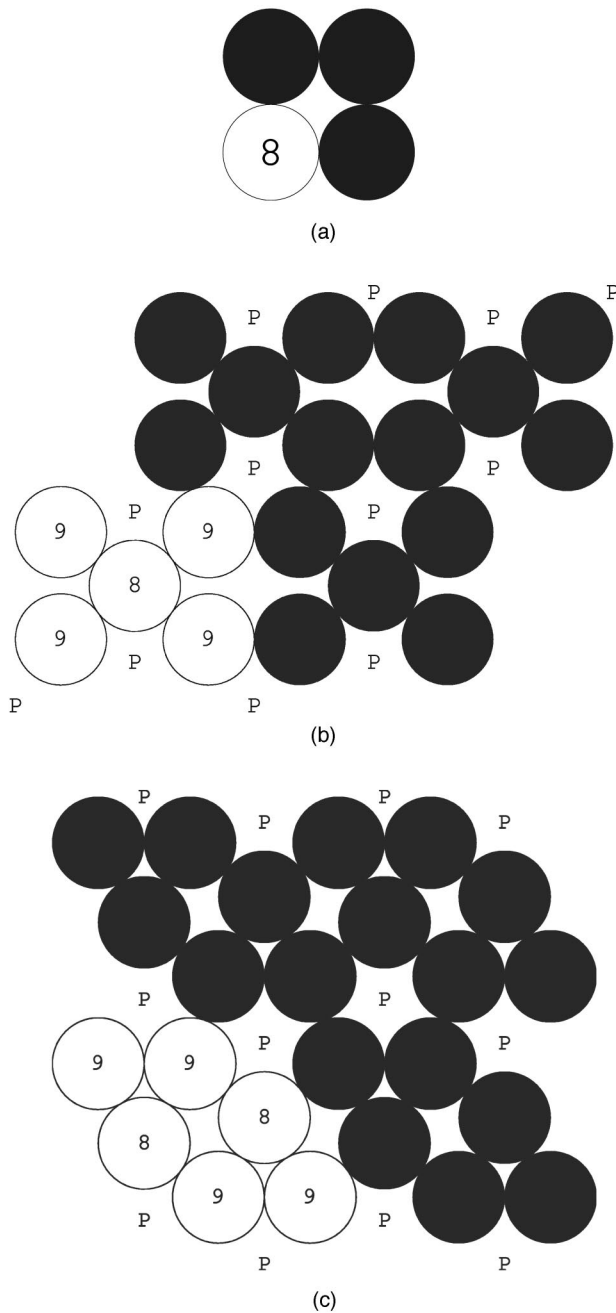


FIG. 2. Repeating segments of the three crystals. (a) In the square crystal, each particle interacts with eight nearest neighbors. (b) In type I pentagonal crystals,  $\frac{1}{5}$  of the particles have eight neighbors and  $\frac{4}{5}$  of the particles have nine neighbors. (c) In type II pentagonal crystals,  $\frac{1}{3}$  of the particles have eight neighbors and  $\frac{2}{3}$  of the particles have nine neighbors. Five particle pentagons, denoted by letter ‘P,’ form the pentagonal crystals. The particles indicated in white are the particles in a basic cell that can be used to construct the crystal by translation; there are, respectively, one, five, and six particles in the unit cell of the square, pentagonal I, and pentagonal II crystals.

stable periodic crystal phases produced by translationally ordering each of the configurations in Fig. 2 and calculate the energies of these crystal structures at  $T=0$ . In our system, the two allowed local configurations are the four-particle square and the five-particle pentagon [indicated by the symbol ‘P’ in Figs. 2(b) and 2(c)]. Particles form these two

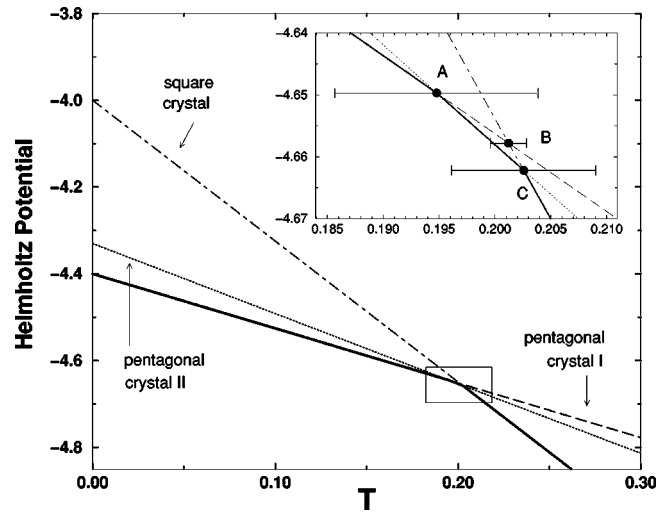


FIG. 3. Helmholtz potentials of pentagonal crystals of type I and II and the square crystal at various temperatures. Points A, B, and C of the inset indicate the intersections of the Helmholtz potential lines at  $T_A=0.195\pm0.010$ ,  $T_B=0.201\pm0.005$ , and  $T_C=0.203\pm0.006$ . The solid line indicates the lowest Helmholtz potential: below  $T_A$  the type I pentagonal crystal is the most stable, between  $T_A$  and  $T_C$  the type II pentagonal crystal is the most stable, and above  $T_C$  the square crystal is the most stable.

geometries because the nearest-neighbor diagonal and adjacent distance between particles in these configurations is less than  $b/a=\sqrt{3}$ , the SW width. Four particle squares make up the square crystal; since each particle has 8 neighbors at  $T=0$ , the potential energy per particle is  $U_{sq}=-4.0$ . Pentagons do not tile the plane; however, the formation of two kinds of crystals based on the local five-particle pentagon is possible. In the type I pentagonal crystal, each crystalline cell consists of five particles, one of which has eight neighbors and four of which have nine neighbors; hence,  $U_{pI}=-4\frac{2}{5}$  [Fig. 2(b)]. In the type II pentagonal crystal, each crystalline cell consists of six particles, two of which have eight neighbors and four of which have nine neighbors; hence,  $U_{pII}=-4\frac{1}{3}$  [Fig. 2(c)]. Since  $U_{pI}<U_{pII}<U_{sq}$ , at our chosen density and low enough temperatures, the type I pentagonal crystal should be the stable phase at  $T=0$  [Fig. 3].

Next, we investigate the stability of the three crystalline phases at  $T>0$  by estimating the Helmholtz potential per particle  $A=U-TS$  in the square crystal and in the pentagonal crystals of type I and type II. Here  $S$  is the entropy. Since our simulations are performed at constant density, we must use the Helmholtz potential instead of the Gibbs potential. We study the system at dimensionless number density  $\rho=a^2N/V\equiv0.857$ . We have simulated a square crystal with  $N=961$ , a pentagonal crystal type I with  $N=1040$ , and a pentagonal crystal type II with  $N=792$ , all at the same  $\rho$ . We checked that at low temperatures,  $T<0.1$ , the potential energy  $U(T)$  is temperature independent, and has the same value as the potential energy of the ideal crystal at  $T=0$ . Hence, we approximate  $U(T)$  at higher  $T$  by  $U(0)$ .

In order to plot the behavior of the Helmholtz potentials of the three crystals for  $T<0$ , we find the entropic contributions  $S$ , by estimating the entropy per particle for each of the

TABLE I. Energy  $U$ , entropy  $S$ , and the Helmholtz potential  $A$  at temperature  $T=0.2$  where the quasicrystal is found.

| Crystal       | $U$             | $S$                | $A(T=0.2)$ |
|---------------|-----------------|--------------------|------------|
| Pentagonal I  | $-4\frac{2}{5}$ | $1.259 \pm 0.028$  | $-4.652$   |
| Pentagonal II | $-4\frac{1}{3}$ | $1.603 \pm 0.0052$ | $-4.654$   |
| Square        | $-4$            | $3.247 \pm 0.021$  | $-4.649$   |

three crystal types. We use the probability density  $p(x,y)$  to find a particle at position  $(x,y)$ . Thus, the entropy is

$$S = \left\langle \int p(x,y) \ln p(x,y) dx dy \right\rangle_{cell}, \quad (1)$$

where the average is taken over every particle in the crystal-line cell. We estimate  $p(x,y)$  by the fraction of the total time  $t$  spent by a particle in a discretized area,  $\Delta x \Delta y$ , at a low enough temperature that the potential-energy fluctuations of the crystalline structure are negligible. The values of the entropies for the three crystals are given in Table I.

Our estimates for the temperature dependence of the Helmholtz potential for the three types of crystals are given in Fig. 3. The condition for stability of the pentagonal crystals is that their Helmholtz potentials,  $A_{pI}$  and  $A_{pII}$ , are lower than the Helmholtz potential of the square crystal,  $A_{sq}$ . In accord with this condition, the square crystal is stable at temperatures above  $T=0.203$ , the type II pentagonal crystal is stable between  $T=0.195$  and  $T=0.203$  and the type I pentagonal crystal is stable below  $T=0.195$ .

While studying the interesting region around  $T \approx 0.2$  (see Fig. 3), we observe the formation of the quasicrystal. We choose to investigate, using MD simulations, our system at  $T \approx 0.2$  because this is the temperature regime where the three crystals have similar values of Helmholtz potential. Cooling the fluid phase, we find the formation of the square crystal below  $T \approx 0.5$ . However, when further cooled into the temperature regime where the Helmholtz potentials of the two pentagonal crystals are lower than the Helmholtz potential of the square crystal, the system does not form pentagonal crystal I or pentagonal crystal II (within our simulation times), but remains as the square crystal. Hence, we use a different approach to try to form the pentagonal crystals: we heat an amorphous phase. We first form the amorphous phase by quenching the system from high to very low temperatures  $T \leq 0.1$ . To do this, we study a system of  $N=961$  [10] particles at  $\rho=0.857$ , which is initially in the fluid phase at high temperature  $T=10$ . We quench this system to  $T=0.1$  and thermalize for  $10^7$  time units [11]. Time constraints prevent us from studying systems with more than 961 particles. Long thermalization times are required to stabilize thermodynamic observables like energy and pressure.

The amorphous phase is a homogeneous mixture of pentagons and squares [Fig. 4(a)]. The lack of long-range structural order in the amorphous phase is evident from the homogeneity of the circles in the isointensity plot [Fig. 4(b)]. When heating the amorphous phase [12] to temperatures above  $T \approx 0.15$ , we find that diffusion becomes sufficient for local rearrangement to occur, and the pentagons begin to coalesce. Instead of forming type I or II pentagonal crystals, the pentagons begin to form rows [Fig. 4(c)] that bend at

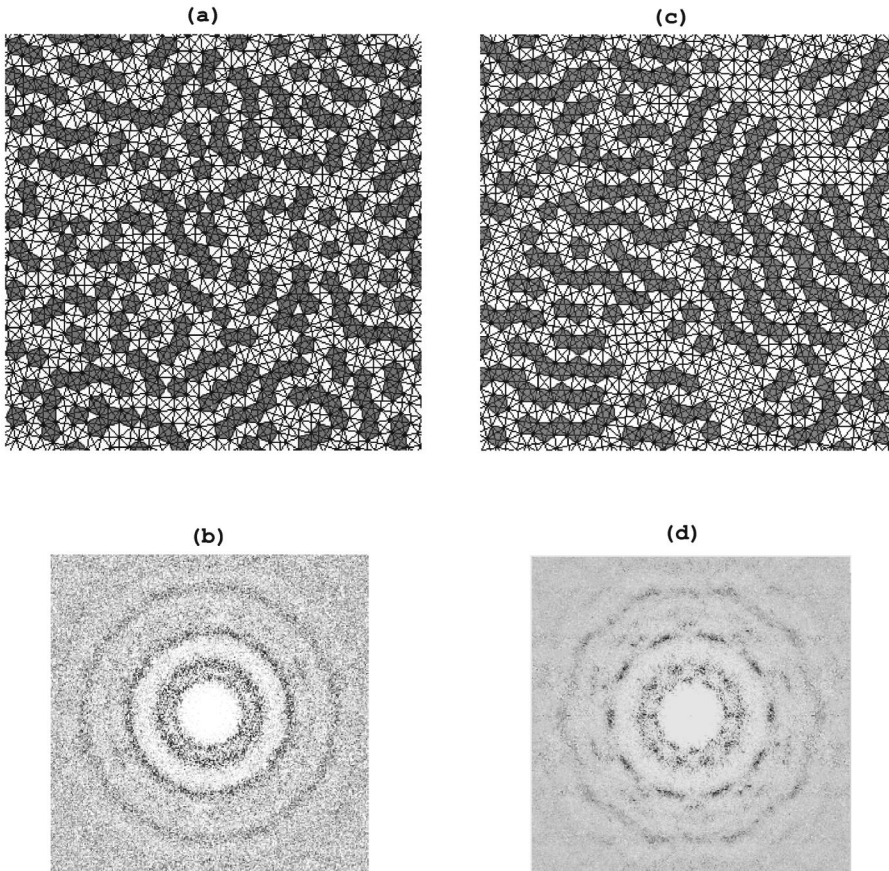


FIG. 4. Amorphous and quasicrystal phases are shown along with their corresponding isointensity plots: the simulated equivalent to a crystallographic diffraction pattern, given by the Fourier transform of the density function: the darkness is proportional to the amplitude of the Fourier transform. On the original system snapshots [(a) and (c)], pentagons are indicated by the shaded areas and lines indicate interacting pairs of particles. (a) Uniformly distributed pentagons in the amorphous phase give rise to the (b) homogeneous rings in the isointensity plot. (c) The pentagons in the quasicrystal phase have coalesced in curved rows that run approximately parallel to one another, in contrast to part (a) where the rows are much less apparent and are not even approximately parallel. (d) The ten isointensity peaks of the quasicrystal.



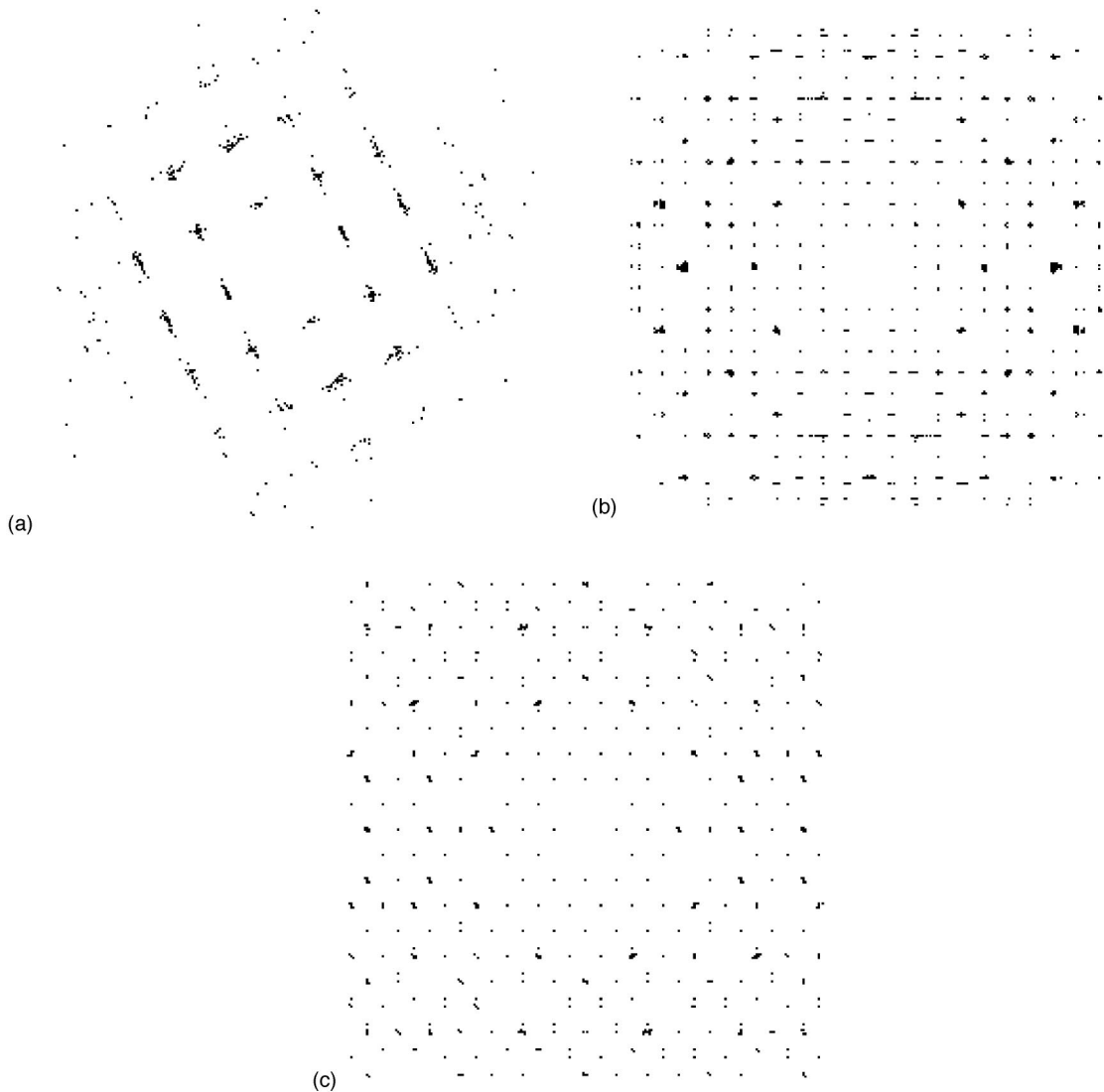


FIG. 5. (a) Square crystal, (b) type I pentagonal crystal, and (c) type II pentagonal crystal isointensity plots.

angles which are multiples of  $36^\circ$ . The angle in the bending of the rows gives rise to the fivefold orientational symmetry, which corresponds to the ten easily observed peaks in the isointensity plot [Fig. 4(d)]. These ten peaks are characteristic of the quasicrystal phase [13], as they are arranged with disallowed fifth-order point-group symmetry [7]. The configuration that we obtain has defects, mainly patches of square crystal, which cause the discontinuity in the rows and lead to the broadening of the diffraction peaks. For comparison, we present in Fig. 5 the isointensity plots of the simulated square and pentagonal crystals. The diffraction patterns illustrate the symmetry of the original crystal system. The four equal sides of the square crystal unit cell [Fig. 2(a)] are clear in the symmetry of the isointensity plot Fig. 5. The isointensity plot of pentagonal crystal I [Fig. 5(b)] shows no hints of anything but well-defined centered-rectangular symmetry [Fig. 2(b)] [14]. The isointensity plot of pentagonal crystal II has mainly a rectangular symmetry that matches the rectangular symmetry of the unit cells [Fig. 2(c)]. Although the two pentagonal crystals are formed from ordered pentagons, their long-range symmetries are four sided. Their

corresponding isointensity plots illustrate these fourfold symmetries, which are distinctly different from the fivefold quasicrystal isointensity plot.

#### IV. QUASICRYSTAL

##### A. Formation

Since the phase transition between the two pentagonal crystals occurs at  $T \approx 0.2$ , we choose this temperature as the one to investigate for quasicrystal formation. After the amorphous phase is quenched to  $T = 0.1$ , we anneal the system at  $T = 0.205$ , for  $2 \times 10^7$  time units, and calculate the diffusion coefficient  $D$ , pressure  $P$  [15], and potential energy  $U$ . We calculate  $D$  using the Einstein relation  $D = (1/2d) \lim_{t \rightarrow \infty} \langle \Delta r(t)^2 \rangle / t$ , where  $d$  is the system dimension. After a short initial period of increase, we observe that  $D$  and  $U$  decrease with time and reach plateaus [Fig. 6]. The diffusion coefficient approaches zero, which is consistent with the possible formation of a quasicrystal phase. The isointensity

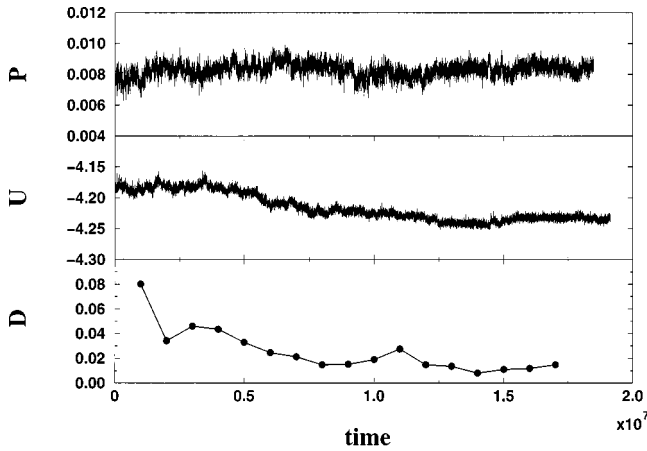


FIG. 6. Behavior of pressure  $P$ , potential energy per particle  $U$ , and diffusion coefficient  $D$  versus time when the system, initially in the amorphous phase, is equilibrated at  $T=0.205$ . The density is  $\rho=0.857$  and the number of particles is  $N=961$ .

peaks also sharpen with the duration of annealing. Due to MD time constraints, we are not sure that we reach the potential energy of a perfect quasicrystal, which is expected to be comparable to the energies,  $U_{pI} = -4\frac{2}{3}$  and  $U_{pII} = -4\frac{1}{3}$ , of the pentagonal crystals. The lowest potential energy reached is  $U_{qc} = -4.25$ .

We observe the spontaneous formation of the quasicrystal phase in the range of temperatures between  $T=0.190$  and  $T=0.205$ . As we heat either the amorphous phase or the quasicrystal above  $T=0.21$ , the square crystal forms, consistent with the Helmholtz potential estimations of Fig. 3.

Next we address the question of whether the quasicrystal phase is stable, by comparing the values of the Helmholtz potential for the three crystal types. As can be seen [Figs. 4(c) and 4(d)], the structure of the quasicrystal arises from the bending rows of pentagons, which locally resemble the pentagonal crystals of either type I or II. We assume that local arrangements of particles corresponding to a square crystal are defects [16] that would be absent in the perfect quasicrystal. If we assume that the local arrangement of the quasicrystal is similar to a combination of the local arrangements in the pentagonal crystal I and the pentagonal crystal II, we can approximate the Helmholtz potential of the quasicrystal by the average Helmholtz potential of the two pentagonal crystals. Because the quasicrystals have a positive entropy contribution to the total entropy due to their degeneracy [3], we add an additional term  $-TS_c$  to the original estimate of the Helmholtz potential energy. Here  $S_c$  is the entropy due to the possible configurations of the quasicrystal.

### B. Entropy

We estimate  $S_c$  as the logarithm of the number of configurations formed by  $n$  pentagons in the quasicrystal. A single pentagon can be oriented in two possible ways when attached side by side to an existing row of pentagons. Neglecting the interaction between adjacent rows, we can estimate the upper bound for the number of configurations as  $2^n$ ,

where  $n$  is the total number of pentagons in the quasicrystal. Note that at point A on Fig. 3, the Helmholtz potentials of both pentagonal crystals coincide, so an additional  $-TS_c$  term should stabilize the quasicrystal in the vicinity of point A.

To better estimate  $S_c$ , we notice that the bending rows of pentagons forming the quasicrystal resemble a compact self-avoiding random walk on the hexagonal lattice. The number of such walks grows as  $Z^n$  where  $Z \approx 1.3$  and  $n$  is the number of steps [17]. Since the formation of one pentagon in the midst of a perfect square crystal lowers the energy of the system by  $U = -1$ , we estimate  $n$  to be  $(U_{qc} - U_{sq})N$ . Assuming that the ground-state energy of the quasicrystal is between  $U_{pI}$  and  $U_{pII}$ , the number of pentagons in the quasicrystal should not be smaller than the number of pentagons in the crystal of type II (which is the pentagonal crystal with the lesser number of pentagons and has  $n = \frac{1}{3}N$ ). We estimate the entropy of configuration per particle to be  $S_c \approx \ln(Z^n)/N = \frac{1}{3} \ln(1.3) = 0.087$ . Thus, the quasicrystal should be more stable than the pentagonal crystals between  $T=0.16$  and  $T=0.23$ , where the gap between the Helmholtz potential of the pentagonal crystals is smaller than the configuration term  $TS_c$ , which ranges from 0.014 to 0.020 in the interval where  $T$  increases from 0.16 to 0.23. Since the  $TS_c$  term lowers the Helmholtz potential of the obtained quasicrystal configuration below the Helmholtz potentials of the two pentagonal crystals, it is likely that the obtained state with fivefold rotational symmetry is not the coexistence of type I and II pentagonal crystals, but is a stable quasicrystalline phase. A more rigorous investigation of this problem would either require the construction of a perfect Penrose tiling [18,19] or of a random tiling [20,21] involving the local structures of crystals type I and II.

## V. DISCUSSION

To summarize, perfect pentagonal crystals of type I and II do not form spontaneously during the time scales of our study. Instead, the quasicrystal, having long-range, fivefold orientational order with no translational order, forms from the coalescence of pentagons present in the starting amorphous phase. The starting amorphous configuration must initially be quenched at a low enough temperature in order to prevent crystallization to the square phase. Moreover, the amorphous phase must be carefully thermalized at the quench temperature, as we have observed that, upon heating a poorly equilibrated amorphous phase with a higher concentration of squares, the system phase separates into regions of pentagons and squares. If the starting amorphous phase does not have a sufficient concentration of pentagons, the quasicrystal will not form: large regions of square crystal will inhibit the long-range order of pentagons and thus not give rise to the ten diffraction peaks in the iso-intensity plot. It is interesting to notice that the bending rows observed in our quasicrystal could resemble the stripe structure of a spinodal decomposition [7]. Anyhow, in the case of spinodal decomposition, the diffraction pattern would be similar to that of an amorphous structure.

Before concluding, we note that Jagla [4], using Monte Carlo simulations, recently reported the existence of quasi-

crystals in a two-dimensional, monodisperse system of hard spheres interacting with a *purely repulsive potential* [4]. The quasi-crystal we observe has a different structure from that modeled by Jagla: our quasicrystal is not a ground-state structure and forms only at nonzero temperature. Also, formation of quasicrystals in monodisperse systems has been observed using complex radially symmetric potentials both in two dimensions [20] and three dimensions [22,23]. To the best of our knowledge, the quasicrystal found in our simulations has a structure different from those previously studied.

## ACKNOWLEDGMENTS

We are very grateful to the late Shlomo Alexander, who pointed out the possibility of the formation of quasicrystals in the square-well potential. We thank R. Hurt and his colleagues at Brown University for encouraging this project in its early stages, and L. A. N. Amaral, C. A. Angell, E. Jagla, K. Ludwig, J. E. McGarrah, C. J. Roberts, R. Sadr, F. Sciortino, F. W. Starr, A. Umansky, and Masako Yamada for helpful interactions. We also thank the U.S. DOE and NSF for financial support.

- 
- [1] D. Shechtman, I. Blech, D. Gratias, and J. W. Cahn, *Phys. Rev. Lett.* **53**, 1951 (1984).
  - [2] M. Widom, K. J. Strandburg, and R. H. Swendsen, *Phys. Rev. Lett.* **58**, 706 (1987).
  - [3] K. W. Wojciechowski, *Phys. Rev. B* **46**, 26 (1992).
  - [4] E. A. Jagla, *Phys. Rev. E* **58**, 1478 (1998).
  - [5] S. Narasimhan and M. V. Jaric, *Phys. Rev. Lett.* **62**, 454 (1989).
  - [6] A. P. Smith, *Phys. Rev. Lett.* **63**, 2768 (1989); S. Narasimhan and M. V. Jaric, *ibid.* **63**, 2769 (1989).
  - [7] P. M. Chaikin and T. C. Lubensky, *Principles of Condensed Matter Physics* (Cambridge University Press, Cambridge, 1995).
  - [8] D. C. Rapaport, *The Art of Molecular Dynamics Simulation* (Cambridge University Press, Cambridge, 1995).
  - [9] In constant-temperature molecular dynamics, the Berendsen method [proposed by H. J. C. Berendsen *et al.*, *J. Chem. Phys.* **81**, 3684 (1984)] can be used to rescale velocities at each time step by a factor  $\chi = [1 + (\delta t/t_T)(T/T - 1)]^{1/2}$ . The current kinetic temperature  $T$  is rescaled towards the desired temperature  $T$  with a rate determined by the time constant  $t_T$ . The time step  $\delta t$  is chosen as a constant parameter of the simulation. In our simulation, the velocity rescaling factor takes the same form, except that  $\delta t$  is the average particle collision interval, during which the velocities of all of the particles are rescaled once. Defining our time constant as  $t_T = \delta t/\kappa$  allows us to control the quench rate by choosing  $\kappa$ .
  - [10] To verify the existence of the quasicrystal, we simulated the same density in a smaller system of 529 particles. At  $T=0.2$ , the ten fivefold diffraction peaks appeared, giving evidence to the formation of the quasicrystalline phase.
  - [11] Time units are defined so that temperature,  $T = \langle m v^2/2 \rangle$ . For our parameters of  $N$ ,  $V$ , and  $T=0.1$ , we find that the average collision interval is approximately one time unit.
  - [12] To form the amorphous phase from the high-temperature liquid, a quench rate of  $\kappa=1$  is used. The amorphous phase is annealed at a slower quench rate of  $\kappa=0.01$ .
  - [13] A. P. Tsai, *MRS Bull.* **22**, 43 (1997).
  - [14] C. Kittel, *Introduction to Solid State Physics* (Wiley, New York, 1996).
  - [15] For  $\rho=0.857$ , pressure at this density is almost constant, as energy continually decreases (Fig. 6). For densities slightly below or above  $\rho=0.857$ , pressure suffers a constant drift during the time scales accessible to our simulations, indicating that the system, at these densities, is further from equilibrium than when  $\rho=0.857$ .
  - [16] Two large defects appear in Fig. 4(c), one at the bottom center and the other in the upper right quadrant.
  - [17] T. M. Birshtein and S. V. Buldyrev, *Polymer* **32**, 3387 (1991).
  - [18] M. Senechal, *Quasicrystals and Geometry* (Cambridge University Press, Cambridge, 1995).
  - [19] C. L. Henley, *Phys. Rev. B* **34**, 797 (1986).
  - [20] A. Quandt and M. P. Teter, *Phys. Rev. B* **59**, 8586 (1999).
  - [21] C. Richard *et al.*, *J. Phys. A* **31**, 6385 (1998).
  - [22] M. Dzugutov, *Phys. Rev. Lett.* **70**, 2924 (1993); J. Roth and M. Dzugutov, *ibid.* **79**, 4042 (1997).
  - [23] A. R. Denton and H. Löwen, *Phys. Rev. Lett.* **81**, 469 (1998).